

The effect of check dams on the dynamic and bed entrainment processes of debris flows

Abstract Bed entrainment plays a significant role in the formational process of a debris flow. Thus the influence of bed entrainment may be an important factor which cannot be neglected when assessing the prevention effect of check dams. However, since few studies have investigated the interaction between check dams and debris flows with considering bed entrainment, the interactive effect of check dams on the dynamic and bed entrainment processes of debris flows remains unclear. Therefore, in this paper, an improved depth-averaged model is proposed to overcome this weakness. In the improved model, the impeding effect of a check dam is simplified as a rigid constraint, and a new computational scheme is adopted to improve the simulation efficiency. Using this model, the dynamic and bed entrainment processes of the catastrophic 2010 Hongchun gully debris flow are analyzed, and the effects of check dams on this debris flow are studied. The results show that the present model can properly depict the dynamic and bed entrainment processes of the Hongchun gully debris flow. Without bed entrainment, the flow quantity tends to decrease gradually from the upstream to the downstream, while the flow quantity will show an opposite tendency if bed entrainment is considered. The check dams can largely reduce the bed entrainment scale and flow quantity of this debris flow. Additionally, the prevention effect of check dams tends to be better when they are constructed at the upper part of the gully by constraining bed entrainment.

Keywords Disaster prevention · Debris flow · Numerical simulation · Check dam · Bed entrainment

Introduction

Debris flows are saturated poorly sorted two-phase flows. These flows are usually characterized by high velocity, huge impact force, and long run-out distance, making them one of the most dangerous landslide types (Jakob and Hungr 2005). As world-wide hazardous phenomena, debris flows can occur in any mountainous areas with steep terrain, channelized path, and sufficient rainfall. Additionally, they are distinct from other types of landslides by periodically occurring in the same channels (Hungr et al. 2014). Due to the above characteristics, debris flows have caused enormous economic loss and casualties to human communities around the world (Evans et al. 2009; García-Martínez and López 2005; Ren 2014; Takahashi 2009).

Generally, debris flows fall into two categories according to their initiation mechanisms, namely landslide-induced debris flows (Iverson et al. 1997; Scott et al. 2001) and runoff-induced debris flows (Berti and Simoni 2005; Hu et al. 2016). For runoff-induced debris flows, apart from intensive rainfall, abundant loose material is also a prerequisite for their formations. The huge earthquake happened in Wenchuan County of China in 2008 triggered thousands of landslides, with a total volume of more than five billion cubic meters (Parker et al. 2011). These landslide

deposits became the main source of loose materials of the runoff-induced debris flows in the earthquake impacted area (Huang and Li 2014; Tang et al. 2012a). As a consequence, the frequency and magnitude of debris flows increased dramatically in this area, while in the meantime the precipitation threshold for triggering a debris flow decreased significantly (Tang et al. 2011; Xu et al. 2012). More seriously, more than 2000 people died or disappeared in some huge debris flow events after the earthquake (Tang et al. 2012a). To mitigate this situation, millions of dollars were allocated by the Chinese government to construct countermeasures such as check dams in some gullies (e.g., the Wenjia and Hongchun gullies). Despite all of these efforts, catastrophic debris flows still occurred due to the inadequate effect of some of these mitigation measures (Chen et al. 2015). Furthermore, since in this area debris flows are expected to occur frequently in 5–15 years after the earthquake (Cui et al. 2011), the risk of occurring catastrophic debris flows is still very high. Therefore, it is an urgent mission and of great importance to develop some useful methods for effectively designing and assessing these mitigation measures.

Currently, experiment and numerical simulation are the two main approaches for studying the dynamics of debris flows. Many experiments (most are flume tests) have been conducted in the past few decades. These tests were mainly utilized in illustrating the initial mechanism (Hu et al. 2016), the dynamic characteristics (Iverson et al. 2010) and the impact forces of debris flows (Armanini 1997; Cui et al. 2015; Wang et al. 2018). Experiments are very useful method in terms of helping scientists understand some basic physics of debris flows, but their drawbacks are also obvious, such as having size effect, being expensive, and being time-consuming. These disadvantages limit their applications in assessing the effect of mitigation measures when the prototype debris flow is huge. In comparison, numerical simulation does not suffer from these weaknesses, making them more suitable for mitigation measure design and assessment. Plenty of numerical models have been proposed for simulating the dynamic process of flow-like motions like debris flows (Crosta et al. 2009; Huang et al. 2015; Hungr and McDougall 2009; Liu and Huang 2006; Liu et al. 2016; Ouyang et al. 2013; Pastor et al. 2009; Pitman and Le 2005; Sassa et al. 2010; Shen et al. 2018a). Additionally, since the substantial influence of bed entrainment on the mobility of flow-like landslides is gradually recognized by researchers in this field (Hungr and Evans 2004; Iverson 2012; Iverson and Ouyang 2015), a growing number of models start to consider bed entrainment either by adopting empirically based or mechanically based entrainment methods (Cuomo et al. 2016; Frank et al. 2015; Liu and He 2016; McDougall and Hungr 2005; Ouyang et al. 2015; Pirulli and Pastor 2012; Shen et al. 2018b). Specially, for runoff-induced debris flows, bed entrainment contributes greatly to their formations. Sometimes most mass in a debris flow may come from entraining loose materials along the path, so under such a circumstance bed entrainment cannot be neglected. Although many

progresses have been made in bed entrainment modeling as mentioned above, these previous studies simulated the bed entrainment process of debris flows in a green field (i.e., without barriers along the path), and few studies considered bed entrainment when assessing the prevention effect of check dams on debris flows. More recently, some researchers have implemented numerical models in studying the effects of artificial barriers on flow-like landslides (Chen et al. 2019; Cuomo et al. 2019; Dai et al. 2017; Gao et al. 2017; Kattel et al. 2018; Liu et al. 2013). These studies mainly focused on exploring the mechanical impacts of debris flows on the structures or the impeding effect of artificial barriers. On the other hand, almost none of them considered bed entrainment in their studies and its interactive influences with debris flow dynamics under the effect of check dams. Therefore, some aspects remain unclear in this field, for instance, how check dams affect the bed entrainment process (which will alter debris flow dynamics in turn), and how to quantify and consider their influence when designing check dams in a debris flow gully with obvious bed entrainment phenomenon, etc.

Based on the above analysis, this paper aims at proposing a simple but efficient method for assessing the effect of check dams on the dynamics of debris flows with taking bed entrainment into account. The present study highlights in extending the application of the depth-averaged models from risk assessment of debris flows on green field to the design of mitigation measures (e.g., check dams). The improved model is able to provide more reasonable guides for constructing check dams in debris flow gullies. In the following sections, the basic principles of the improved method are introduced first. Then it is applied in modeling the dynamic process of the catastrophic Hongchun gully debris flow in southwest China. Totally 20 groups of simulations representing different scenarios are conducted to explore the influences of check dams on the bed entrainment and dynamic processes of this debris flow. Afterwards, the simulation results are presented and discussed in detail, and finally, conclusions are drawn according to the results.

Basic principles of the method

Governing equations

The governing equations adopted in this paper consist of one continuity equation and two momentum equations. These equations are deduced according to the mass and momentum conservations of a small rectangular soil column in a Cartesian coordinate system. Bed entrainment is incorporated into these equations as a source term. For simplicity, these equations are only briefly introduced here, and detailed derivations can be found in Shen et al. (2018a). The governing equations are given by,

$$\frac{\partial h}{\partial t} + \frac{\partial Q_x}{\partial x} + \frac{\partial Q_y}{\partial y} - E_r = 0 \quad (1)$$

$$\begin{aligned} \frac{\partial Q_x}{\partial t} + \frac{\partial Q_x^2/h}{\partial x} + \frac{\partial Q_x Q_y/h}{\partial y} = & - \left(k_x h g \frac{\partial h}{\partial x} + g \frac{h^2}{2} \frac{\partial k_x}{\partial x} \right) \\ & + (Ag + B) \frac{h \tan \alpha}{\tan^2 \alpha + \tan^2 \beta + 1} - \frac{\tau_b A_b h v_x}{m \sqrt{v_x^2 + v_y^2 + v_z^2}} \end{aligned} \quad (2)$$

$$\begin{aligned} \frac{\partial Q_y}{\partial t} + \frac{\partial Q_x Q_y/h}{\partial x} + \frac{\partial Q_y^2/h}{\partial y} = & - \left(k_y h g \frac{\partial h}{\partial y} + g \frac{h^2}{2} \frac{\partial k_y}{\partial y} \right) \\ & + (Ag + B) \frac{h \tan \beta}{\tan^2 \alpha + \tan^2 \beta + 1} - \frac{\tau_b A_b h v_y}{m \sqrt{v_x^2 + v_y^2 + v_z^2}} \end{aligned} \quad (3)$$

where h is the thickness of the debris flow, $Q_x = v_x h$ and $Q_y = v_y h$ are the flow quantities in the x and y directions, respectively, v_x and v_y are the flow velocities in the x and y directions, respectively, E_r is the entrainment rate, k_x and k_y are the lateral pressure coefficients in the x and y directions, respectively, which evolve according to the pressure state (active state or passive state) of the soil (Ouyang et al. 2013; Savage and Hutter 1989), g is the gravitational acceleration, A and B are the parameters related to the static and centrifugal supporting forces, respectively, α and β are the dip angles of the sliding mass in the x and y directions, respectively, τ_b is the basal shear stress, A_b is the area of the bottom surface of the soil column, and m is the mass of the soil column. The expressions of A , B and A_b are given by.

$$A = 1 + \left(k_x \frac{\partial h}{\partial x} + \frac{h}{2} \frac{\partial k_x}{\partial x} \right) \tan \alpha + \left(k_y \frac{\partial h}{\partial y} + \frac{h}{2} \frac{\partial k_y}{\partial y} \right) \tan \beta \quad (4)$$

$$B = \frac{C_x}{\cos \alpha} \left(\frac{v_x}{\cos \alpha} \right)^2 + \frac{C_y}{\cos \beta} \left(\frac{v_y}{\cos \beta} \right)^2 \quad (5)$$

$$A_b = dx dy \sqrt{\tan^2 \alpha + \tan^2 \beta + 1} \quad (6)$$

where C_x and C_y are the curvature of the bed in the x and y directions, respectively, dx and dy are the sizes of the soil column in the x and y directions, respectively.

In some models, two additional momentum production terms ($E_r v_{bx}$ and $E_r v_{by}$) may appear in the momentum equations (Eqs. (2)–(3)). However, since the erodible mass are usually assumed to be static ($v_{bx} = v_{by} = 0$) before being entrained, these momentum productions terms are removed from the momentum equations in this paper.

Rheological law and entrainment model

The governing equations are not closed before E_r and τ_b are determined by some kinds of models. The widely used Voellmy model is adopted to calculate the basal shear stress of the debris flow.

$$\tau_b = \sigma(1 - r_{ub}) \tan \phi_s + \rho_s g \frac{v_x^2 + v_y^2}{\xi} \quad (7)$$

where σ is the normal stress on the bed, r_{ub} is the pore water pressure coefficient on the bed, ϕ_s is the effective friction angle of the debris flow, ρ_s is the bulk density of the debris flow, and ξ is the turbulence coefficient. To determine E_r , a mechanically based model proposed by Fraccarollo and Capart (Fraccarollo and Capart 2002) is adopted given it has clear physical meaning

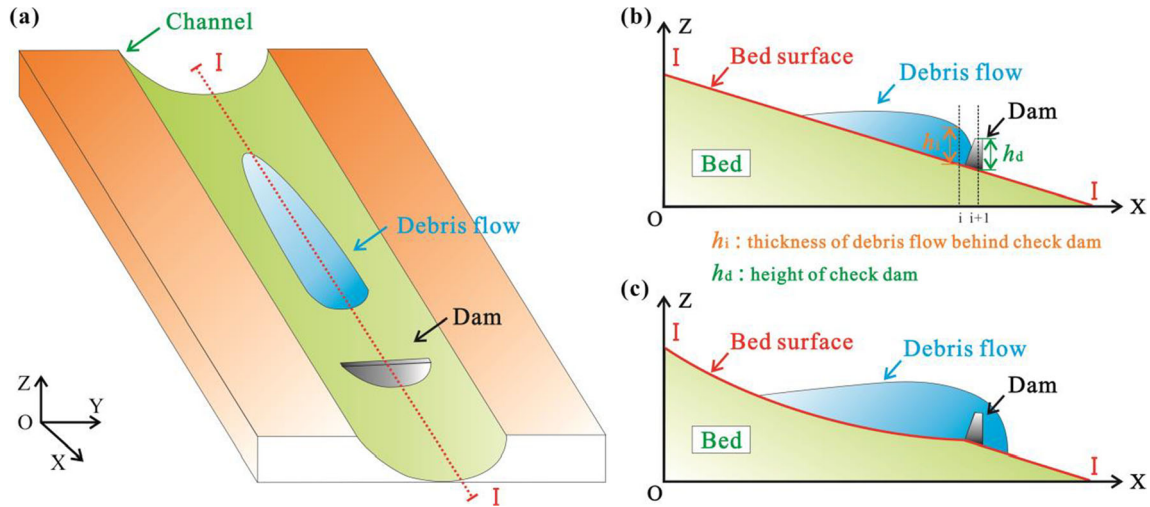


Fig. 1 Schematic diagram of the interaction between channelized debris flow and check dam. **a** Three-dimensional view before interaction, **b** result after interaction without entrainment, and **c** result after interaction with entrainment

$$E_r = -\frac{\partial Z}{\partial t} = \frac{\tau_b - \tau_e}{\rho_e \sqrt{v_x^2 + v_y^2}} \quad (8)$$

where Z is the elevation of the bed, τ_e is the resistant shear stress in the erodible mass, and ρ_e is the bulk density of the erodible mass. τ_e is calculated according to the Mohr-Coulomb model

$$\tau_e = \sigma(1 - r_{ue})\tan\phi_e + c_e \quad (9)$$

where r_{ue} is the pore water pressure coefficient in the erodible mass, ϕ_e is the effective friction angle of the erodible mass, and c_e is the cohesion of the erodible mass. Substituting Eq. (7) and (9) into Eq. (8), the following entrainment model can be obtained

$$E_r = -\frac{\partial Z}{\partial t} = \left(\sigma(1 - r_{ub})\tan\phi_s + \rho_s g \frac{v_x^2 + v_y^2}{\xi} - \sigma(1 - r_{ue})\tan\phi_e - c_e \right) \frac{1}{\rho_e \sqrt{v_x^2 + v_y^2}} \quad (10)$$

Equation (10) is utilized to determine the entrainment rate in this paper. This equation is similar to the entrainment model adopted in Ouyang et al. (2015), and it takes advantages of both the Voellmy model and the Mohr-Coulomb model.

Constraint of check dams and computational scheme

To reflect the restraining impact of check dams on debris flows, check dams are taken as a kind of rigid constraint, as shown in Fig. 1. Therefore, the failure of check dams is not considered in the present study. Those computational cells with a dam inside are marked, and their neighboring cells are also identified. Assuming the height of the dam is h_d and the thickness of the debris flow in an cell next to the dam (at the upstream side, see Fig. 1b) is h_i , then the following velocity constraint is imposed to the upstream cells next to the dam

$$v = \begin{cases} 0 & \text{if } h_i < h_d \\ \text{calculate value} & \text{if } h_i \geq h_d \end{cases} \quad (11)$$

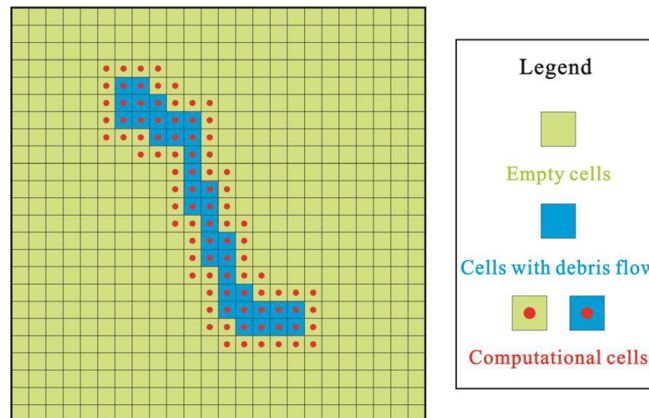


Fig. 2 Dynamic computational cells used in the model to reduce computational consumption

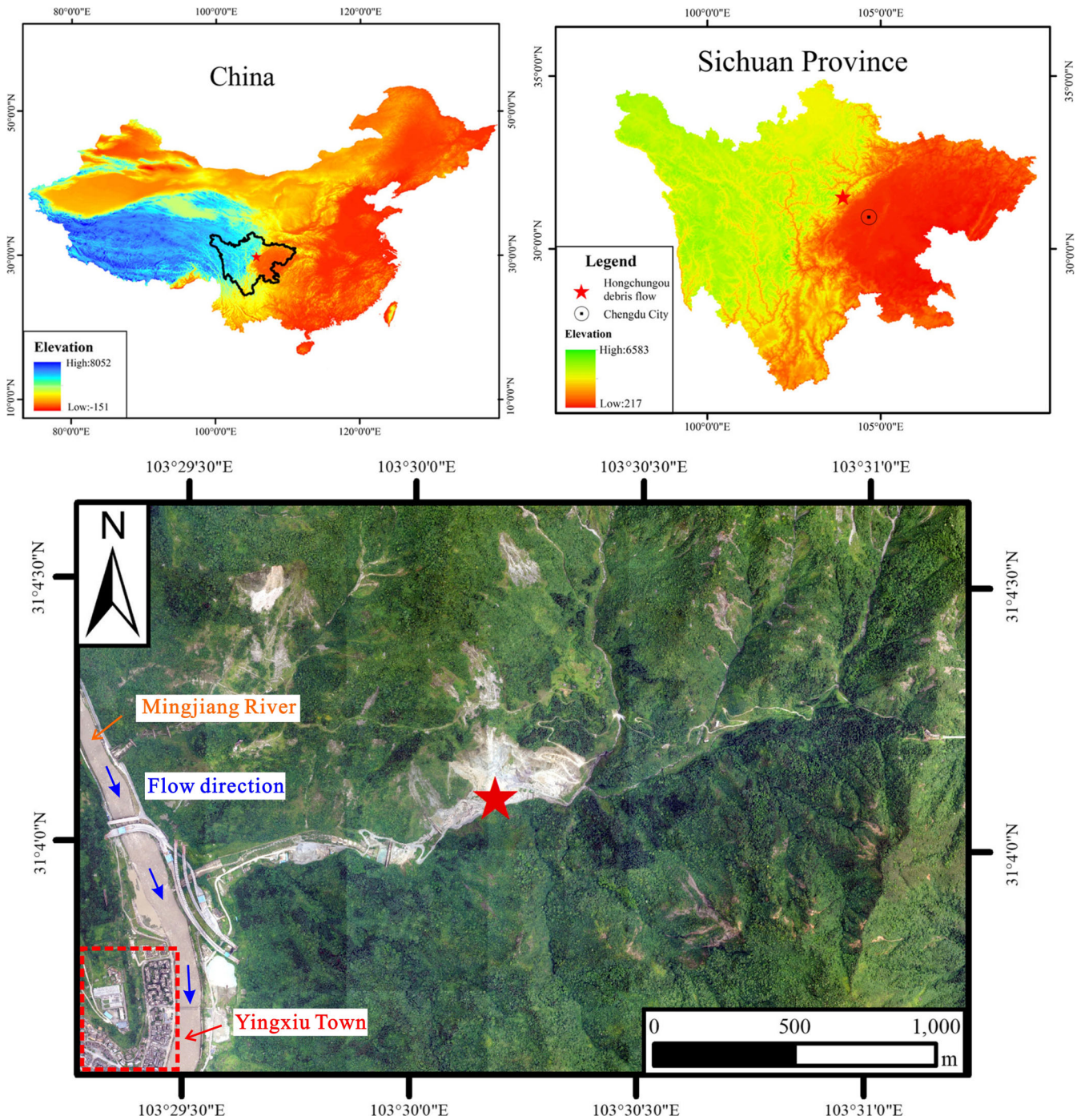


Fig. 3 Location of the Hongchun gully in China (N 31°04'01.1", E 103°29'32.7")

Equation (11) implies that when the thickness of the debris flow is lower than the height of the dam, it will not be able to flood over the top of the dam. In this situation, the debris flow will accumulate behind the dam, until it becomes thick enough to surpass the dam to a certain extent. By this way, the impeding effect of the dam can naturally be reflected. Figure 1 also schematically illustrates the importance of considering bed entrainment. The outcomes are likely to be totally different when considering or not considering bed entrainment. As illustrated by Fig.1, the outcome

without considering bed entrainment shows that the check dam succeeds in preventing the debris flow (Fig. 1b), while the result of that considering entrainment is totally opposite (Fig. 1c). Therefore, it is necessary to take bed entrainment into account when assessing the effect of check dams.

Noticeably, debris flows usually propagate along long, narrow and meandering gullies. Therefore, only a small area in the channels is occupied by the debris mass. However, when simulating the dynamic process of a huge debris flow, a large rectangular computational region

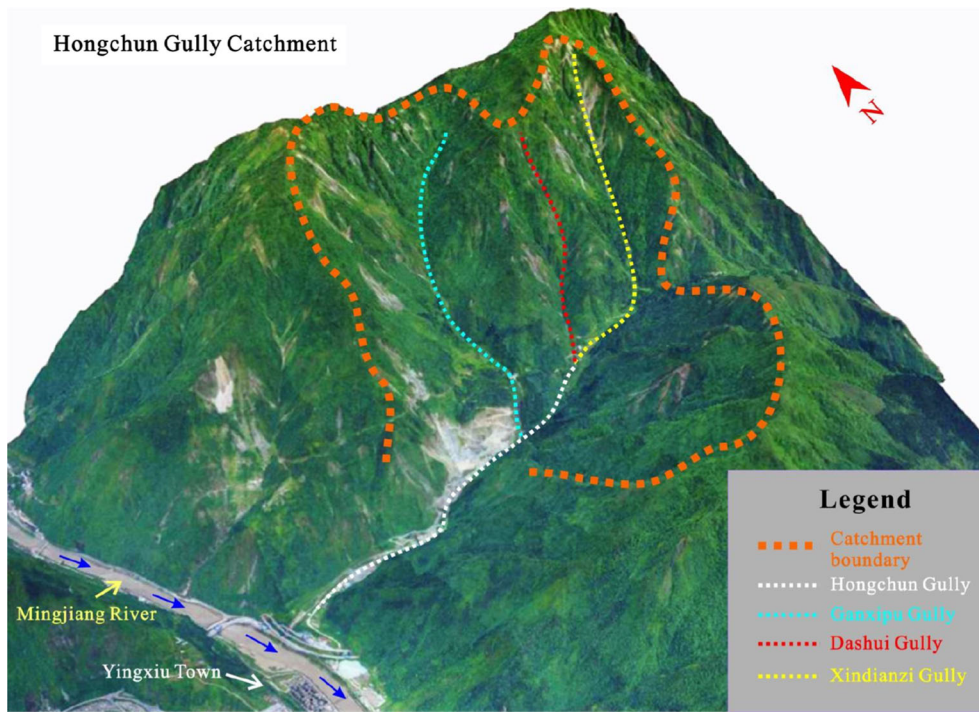


Fig. 4 Panorama of the Hongchun gully catchment

which should contain all the debris flow gullies is usually selected for conducting the simulation. This means that most cells in the computational region are empty and theoretically unnecessary to participate in calculation. In the traditional computational scheme (Ouyang et al. 2013; Shen et al. 2018a), most of these cells still involve in calculation, resulting in a large waste of computational resources and times. To make the model more suitable for simulating huge debris flows, an improved computational scheme is adopted in this paper, as shown in Fig. 2. In the new scheme, the computational cells evolve automatically

according to the propagation of a debris flow. Only those cells with debris mass inside participate in the simulation. This method could reduce the computational effort to almost the minimum level, and it can easily achieve by applying the following logical condition

$$\text{condition} = \begin{cases} \text{skip} & \text{if } h(i, j) = 0 \text{ and with empty neighbors} \\ \text{calculate} & \text{if otherwise} \end{cases} \quad (12)$$

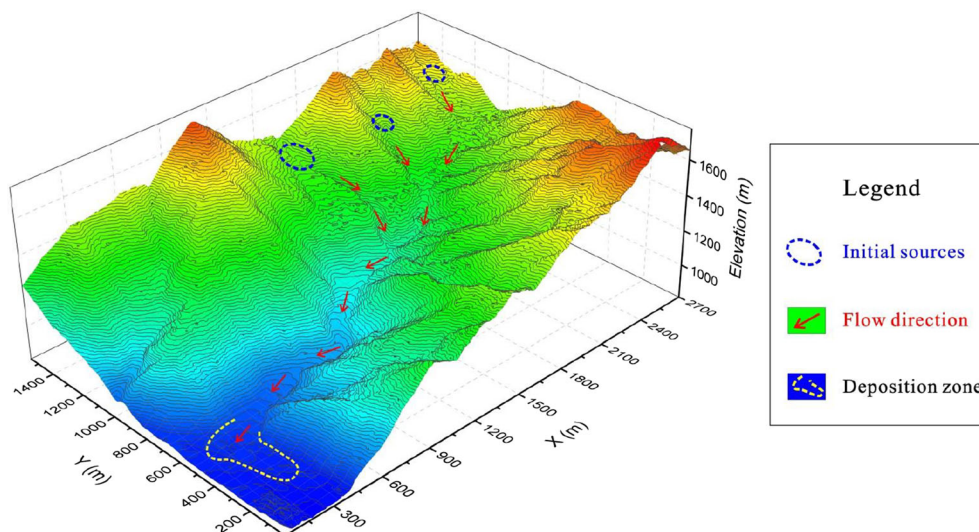


Fig. 5 3D digital elevation model, coordinates setup and initial debris mass distributions in the simulation

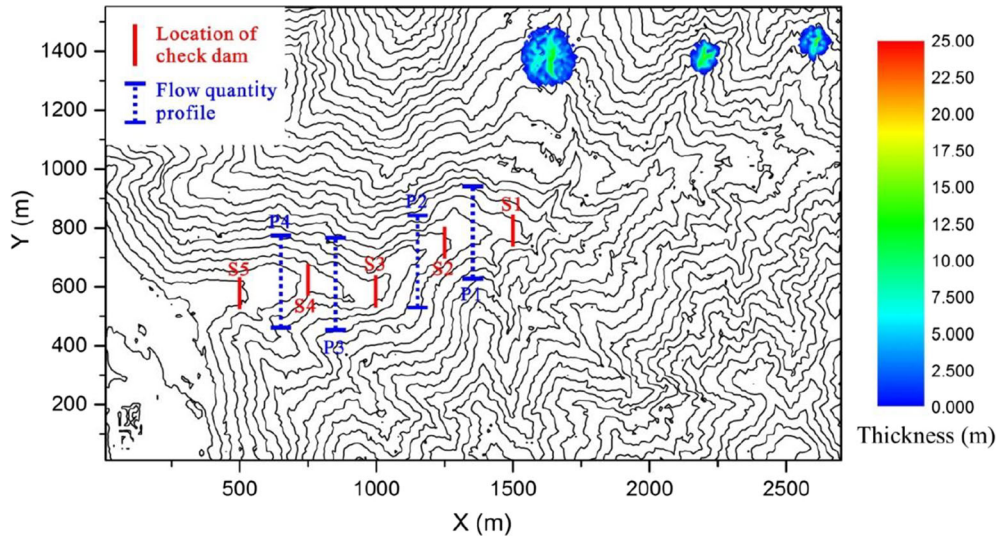


Fig. 6 Locations of the check dams and the profiles for monitoring flow quantity

Equation (12) indicates that all those empty cells whose all neighbors are also empty will be skipped in the calculation.

The constraint of the check dam and the new computational scheme are incorporated into a modified finite difference code developed by Shen et al. (2018a, b) to formulate an improved depth-averaged model. This improved model is designed for modeling long run-out debris flows with accounting for the influences of bed entrainment and check dams, and it is applied in modeling the following debris flow case.

Modeling of the Hongchun gully debris flow

Introduction of the Hongchun gully debris flow

The Hongchun gully is a debris flow gully about 500 m to the northeast of the Yingxiu Town — the epicentral zone of the 2008 huge Wenchuan earthquake, as shown in Fig. 3. The outlet of the gully is next to the Mingjiang River, and the Yingxiu Town is located at the west bank of the river.

During August 12 to 14, 2010, this region experienced a heavy rainfall event with an accumulative precipitation of 162.1 mm (Xu et al. 2012). This rainfall finally triggered hundreds of channelized debris flows (Tang et al. 2012b) near the Yingxiu Town. Among them, the Hongchun gully debris flow occurred on August 14 at 3 a.m. may be the most disastrous one in terms of its huge scale and serious consequence. This debris flow was initiated by the runoff erosion of the landslide deposits in the three branch channels of the Hongchun gully. An estimated total volume of 700,000–800,000 m³ of debris mass involved in this event, and about half of the debris mass (350,000–400,000 m³) rushed out the outlet of the gully and blocked the Mingjiang River. As a consequence, the Mingjiang River changed its course, causing a flood in the newly

reconstructed Yingxiu Town (Tang et al. 2011) and the deaths or disappearances of 17 people.

Figure 4 is the panorama of the Hongchun gully catchment. The total area of this catchment is 5.35 km², and the length of the main gully is about 3.6 km. The elevation of the gully is between 880 m and 1700 m, and it has an average slope gradient of about 36%. The upstream of the Hongchun gully consists of three branch channels. They are the Ganxipu gully, the Dashui gully and the Xindianzi gully from west to east, respectively. All these gullies involved in the August 14 event (Ouyang et al. 2015), and the initial volumes of the debris mass in these three gullies were 112,000 m³ (Ganxipu gully), 39,000 m³ (Dashui gully), and 32,000 m³ (Xindianzi gully), respectively. Therefore, the initial total volume of this debris flow was estimated to be about 183,000 m³, and about 517,000–617,000 m³ of debris mass was entrained along the path. Field survey shows that the phenomenon of bed entrainment is very obvious along the gully, and a maximum entrainment depth of about 20 m occurred in this gully (Ouyang et al. 2015).

Simulation set-ups

A digital elevation model (DEM) with a resolution of 10 m is built up according to the surveying data. The DEM, coordinates setup, and initial distributions of debris mass in the simulation are illustrated in Fig. 5. The computational region is 2700 m in the x direction and 1550 m in the y direction. The sizes of cells in both the x and y directions are 10 m. The maximum time step for simulating this case is 0.02 s.

To study the influence of check dam location on the dynamic and entrainment processes of the Hongchun gully debris flow, five locations along the main gully are selected as the possible locations for constructing check dams. These locations represent five

Table 1 Locations of check dams

Dam location	S1	S2	S3	S4	S5
Center coordinates	X = 1500 m Y = 780 m	X = 1250 m Y = 740 m	X = 1000 m Y = 580 m	X = 750 m Y = 620 m	X = 500 m Y = 570 m

Table 2 Locations of profiles for monitoring flow quantity

Profile	P1	P2	P3	P4
Location	X = 1350 m	X = 1150 m	X = 850 m	X = 650 m

different scenarios of check dam setups: constructing at upper gully, upper and middle gully, middle gully, middle and lower gully, and lower gully, respectively. Four profiles are selected to monitoring the changes of flow quantity under the effect of check dams. The locations of check dams and monitoring profiles are illustrated in Fig. 6, and their coordinates are given in Tables 1 and 2, respectively.

Totally 20 groups of simulations are conducted, and the simulation setups for all these groups are listed in Table 3. Among them, NE and WE represent the situations before constructing check dams, and they are used to calibrate the rheological parameters and analyze the influence of bed entrainment on the August 14 debris flow event. All other groups represent the situations with imaginary check dams, and they are utilized to explore the possible influences of check dams on the dynamic and entrainment processes of this debris flow.

The parameters adopted in these simulations are given in Table 4. Among these parameters, the value of the basal frictional angle, turbulent coefficient (its value here corresponds to a Chezy coefficient value of 12), internal frictional angle and bulk density of the Hongchun gully debris flow are given according to Ouyang et al. (2015). The erodible mass is assumed to have similar property

with the debris flow, so its basal friction angle and bulk density values take the same values as those of the debris flow. The pore pressure coefficient r_u represents the ratio of the pore pressure to the total stress in the soil. However, the pore pressure in a debris flow is usually much larger than the static pore water pressure because excess pore water pressure will generate in the rapid motion. The value of the pore pressure coefficient takes 0.8 for the debris flow, which is a typical value according to debris flow experiments. A relatively higher pore pressure coefficient value is allocated to the erodible mass given it tends to be in undrained condition under rapid shear action. In addition, a small cohesion value is given to the erodible mass to prevent materials on steep slopes being entrained (Ouyang et al. 2015).

Simulation results

Simulation results of the August 14 event

The simulated run-out processes of the debris flow in group NE and WE are shown in Fig. 7. The simulated distributions of debris mass at two times are compared. These two times represent the middle and final stages of the debris flow motion, respectively. At $t = 100$ s, the run-out distance in WE is obviously larger (about 200 m) than that in NE, indicating than bed entrainment

Table 3 Setups in different simulation groups

Simulation groups	Entrainment	Dam numbers	Dam height	Dam position
NE	No	0	–	–
WE	Yes	0	–	–
G0	No	1	20 m	S2
G1	Yes	1	10 m	S1
G2	Yes	1	10 m	S2
G3	Yes	1	10 m	S3
G4	Yes	1	10 m	S4
G5	Yes	1	10 m	S5
G6	Yes	1	20 m	S1
G7	Yes	1	20 m	S2
G8	Yes	1	20 m	S3
G9	Yes	1	20 m	S4
G10	Yes	1	20 m	S5
G11	Yes	2	20 m	S1 and S3
G12	Yes	2	20 m	S1 and S4
G13	Yes	2	20 m	S1 and S5
G14	Yes	2	20 m	S2 and S4
G15	Yes	2	20 m	S2 and S5
G16	Yes	2	20 m	S3 and S5
G17	Yes	3	20 m	S1, S3, and S5

Table 4 Parameters used in simulating the Hongchun gully debris flow

Parameters	Pore pressure coefficient r_u	Basal friction angle ϕ (°)	Turbulent coefficient ξ	Basal cohesion c (kPa)	Internal friction angle ϕ_i (°)	Bulk density ρ (g/cm ³)
Debris mass	0.8	12	2850	–	35	2.02
Erodible mass	0.95	12	–	2.1	–	2.02

significantly facilitates the motion of this debris flow. In addition, the thickness of the debris flow along the main gully in WE (Fig. 7c) is also much thicker than that of NE (Fig. 7a), which means that a noticeable expansion of the scale of the debris flow occurs due to entrainment. At $t=1000$ s, the main propagation process has finished in both WE and NE, but the simulated final deposits of

them show totally different characters. Although the debris flow rushes out from the outlet in both situations, the volume of the rushing out debris mass in WE (about 349,000 m³, see Fig. 7d) is about ten times as much as that in NE (about 35,000 m³, see Fig. 7b). Without considering bed entrainment, the debris flow turns out to be incapable of blocking the Mingjiang River. In

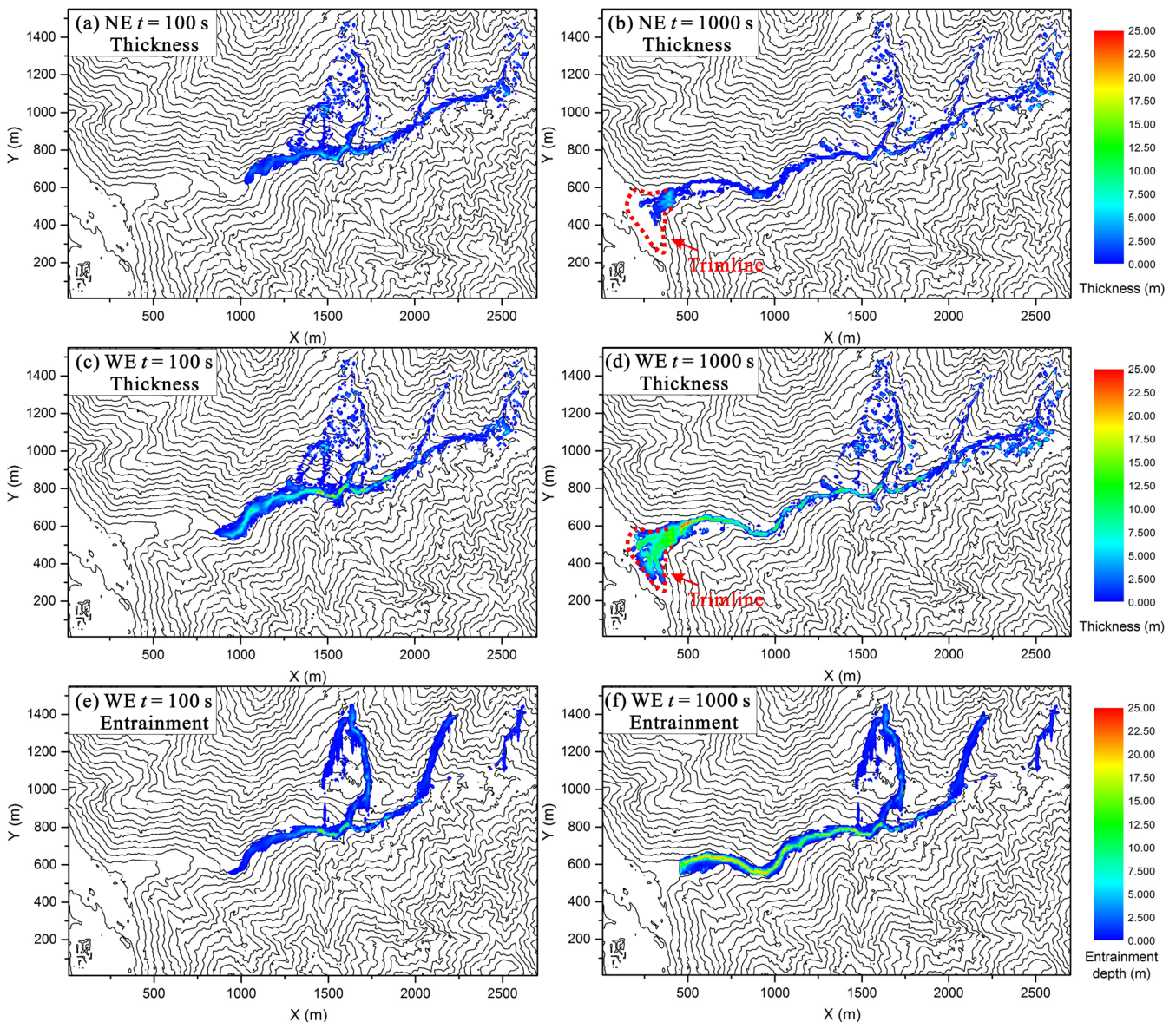


Fig. 7 Simulated deposition and entrainment processes without check dams. **a** and **b** are the thicknesses of debris flow at $t=100$ s and 1000 s without considering entrainment (NE), respectively, **c** and **d** are the thicknesses of debris flow at $t=100$ s and 1000 s considering entrainment (WE), respectively, and **e** and **f** are the entrainment depths at $t=100$ s and 1000 s, respectively

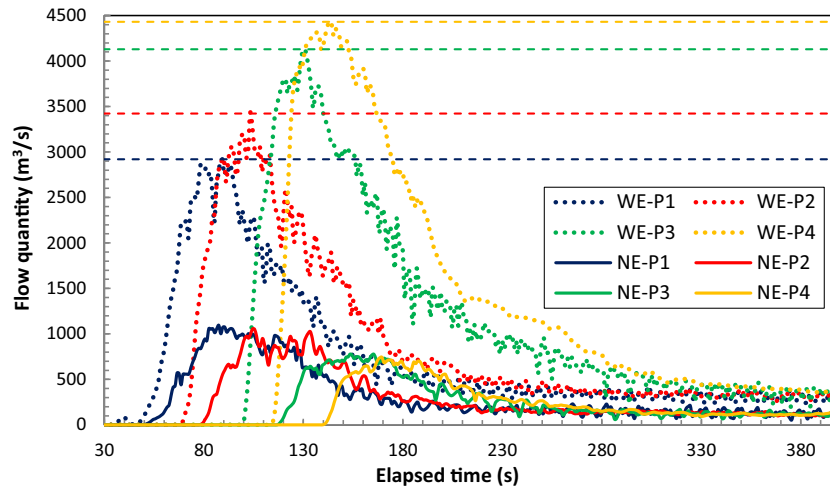


Fig. 8 Simulated flow quantities at four profiles along the gully without check dams, WE: considering bed entrainment, NE: without bed entrainment

comparison, the simulated final deposit considering bed entrainment matches quite well with the measured data in terms of run-out distance, covering area, and the shape and thickness (about 5–10 m) of the debris dam. The entrainment depths in WE at the two times are also presented in Fig. 7. It shows that the peak entrainment depth (about 20 m) appears at the bottom of the main gully, while the entrainment depth decreases gradually from the gully

bottom to the lateral slopes. According to field observation, the most apparent bed entrainment occurred in the middle section of the main gully, with an average thickness of 6–10 m and the maximum depth about 20 m (Ouyang et al. 2015), while the entrainment depth in the three branch gullies are relatively insignificant with an average thickness of only 1–2 m. The simulated entrainment distribution (Fig. 7d) shows good accordance with

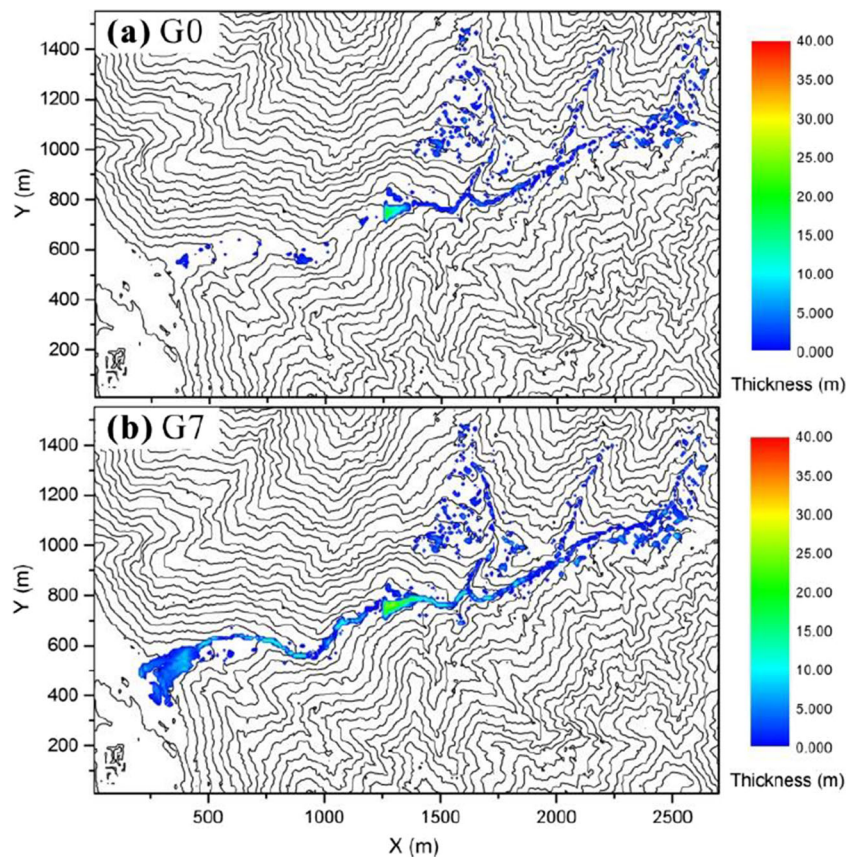


Fig. 9 Comparison of the prevention effect of check dam between G0 (with a 20 m check dam at S2 and without entrainment) and G7 (with a check dam 20 m high at S2 and considering entrainment)

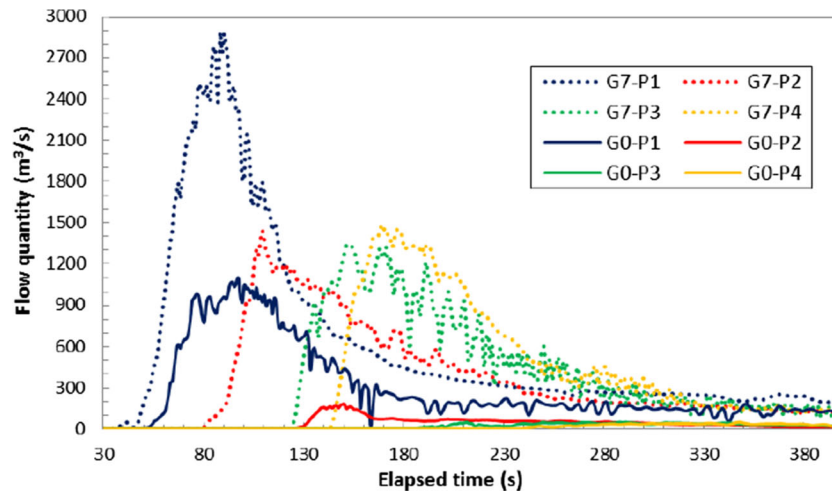


Fig. 10 Comparison of the flow quantities at four profiles between G0 (not considering entrainment) and G7 (considering entrainment)

this observation. The final volume of the debris flow reaches $763,000 \text{ m}^3$, this value also agrees well with the estimated final volume of $700,000 \text{ m}^3$ to $800,000 \text{ m}^3$. The above analysis indicates the improved model adopted here can properly depict the entrainment process of the Hongchun gully debris flow, and the simulation accuracy is quite good.

The simulated flow quantities at the four monitoring profiles in these two groups are compared in Fig. 8. The results of the two groups show totally opposite patterns. When considering bed entrainment, the peak flow quantity values increase gradually from upstream to downstream. This is because the thickness of the debris flow grows quickly by entraining loose materials. However, the peak values show a decreasing tendency when without obtaining new mass by entrainment, because in this situation the thickness of the debris flow is likely to become thinner at downstream. In general, it illustrates that bed entrainment boosts the magnitude of the flow quantity by 3 (P1) to 6 (P4) times in this gully. Additionally, in WE the arrival times of the debris flow at the four profiles are also earlier than their counterparts in NE, which means the debris flow will run faster under the influence of bed entrainment.

Simulation results with the effect of check dam

The results of G7 and G0 are compared first to check the influence of check dam on the dynamic process of this debris flow in the situations considering and not considering bed entrainment. In G7 and G0, a check dam (20 m high) is built up at the upper and middle gully (S2). The results show that in both groups the check dam has an obvious impeding effect on the debris flow, but their outcomes are different. When neglecting bed entrainment (G0, see Fig. 9a), the check dam is shown to perform quite well in preventing the debris flow. Although a small volume of debris mass overrides the dam, almost no debris mass rushes out the outlet. However, an opposite conclusion is illustrated by the result of considering entrainment (G7). In spite of a large amount of the debris mass has been resisted by the dam, the rest debris mass surpassed the dam still turns into a relatively large debris flow by entrainment. The results above indicate that the prevention effect of a check dam is likely to be overestimated if the bed entrainment is not taken into account, which may result in the inadequate design of prevention measures.

The flow quantities at the monitoring profiles in G0 and G7 are compared in Fig. 10. The results show that check dam can significantly reduce the flow quantity of the debris flow at the downstream side of the dam in both situations. In G7, the flow quantity of the debris flow decreases sharply first when it passes the dam under the hindering effect, and then its value increases gradually after surmounting the dam due to entrainment. This explains why the final scale of the debris flow is still big despite a great amount of debris mass has been stopped by the dam. However, the results of G0 show that the flow quantity continuously decreases after overriding the dam.

To further investigate the influence of the locations of check dams on the dynamic and bed entrainment processes of this debris flow, the simulation results of different situations with single dam and multiple dams constructing at different locations are analyzed and presented (Fig. 11).

Figure 11a–c are the results of the situations with one check dam of 20 m high located at S1 (upper gully), S3 (middle gully) and S5 (lower gully), respectively. The performance of the check dam is best when it is located at downstream. Two factors are likely to contribute to this result. The first one is that the velocity of the debris flow at downstream is relatively smaller than that at upstream. Another reason is that the topography at downstream is wider and plainer, so the volume capacity of the check dam is larger than that at upstream. The result of G8 is the worst. This is because the volume capacity of the check dam reservoir at the middle stream is not big, while at the same time the velocity of debris flow is relatively high. In comparison, the check dam achieves a modest effect because it constrains the entrainment scale of the debris flow by reducing the flow quantity at an early stage.

The results of multiple dams (Fig. 11d–h) show similar patterns. When the check dams are constructed at relatively upper parts of the gully (G11 and G14), the prevention effect tends to be better than other situations (G16 and G13) due to the scale of bed entrainment is effectively constrained by the dams. In contrast, the prevention effects of check dams constructing at relatively lower parts of the gully (G16 and G13) is relatively weak, since the scale of the debris flow has already boosted by entraining the loose materials at upstream.

In order to show the impact of check dam on the final entrainment scale of the debris flow, the simulated entrainment depths in

G6, G10, and G11 are presented in Fig. 12. The results agree with the above analysis that constructing check dam at upstream performs better in controlling the final entrainment scale.

The flow quantities at the monitoring profiles in G6, G8, G10, and G14 are compared to reveal the influence of check dam on the flow

quantity of this debris flow (Fig. 13). In these situations, the constraining effect of check dam significantly reduces the magnitude of the flow quantity at the downstream of the dam. This reducing effect tends to be stronger when the dam is located at upstream (Fig. 13c) rather than at middle stream (Fig. 13b) and downstream (Fig. 13a).

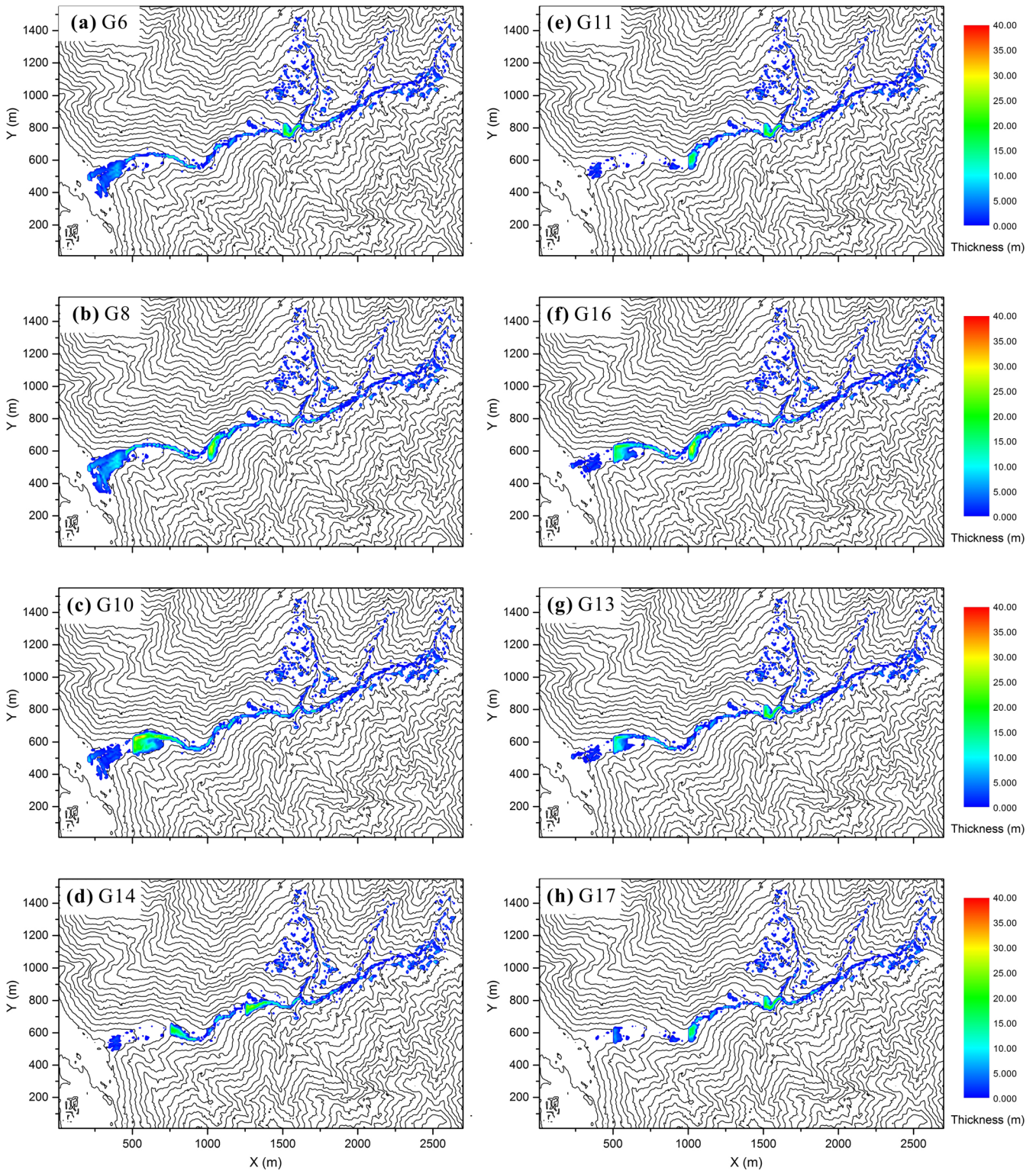


Fig. 11 Simulated final thickness of the debris deposit under the influence of check dam in several different situations

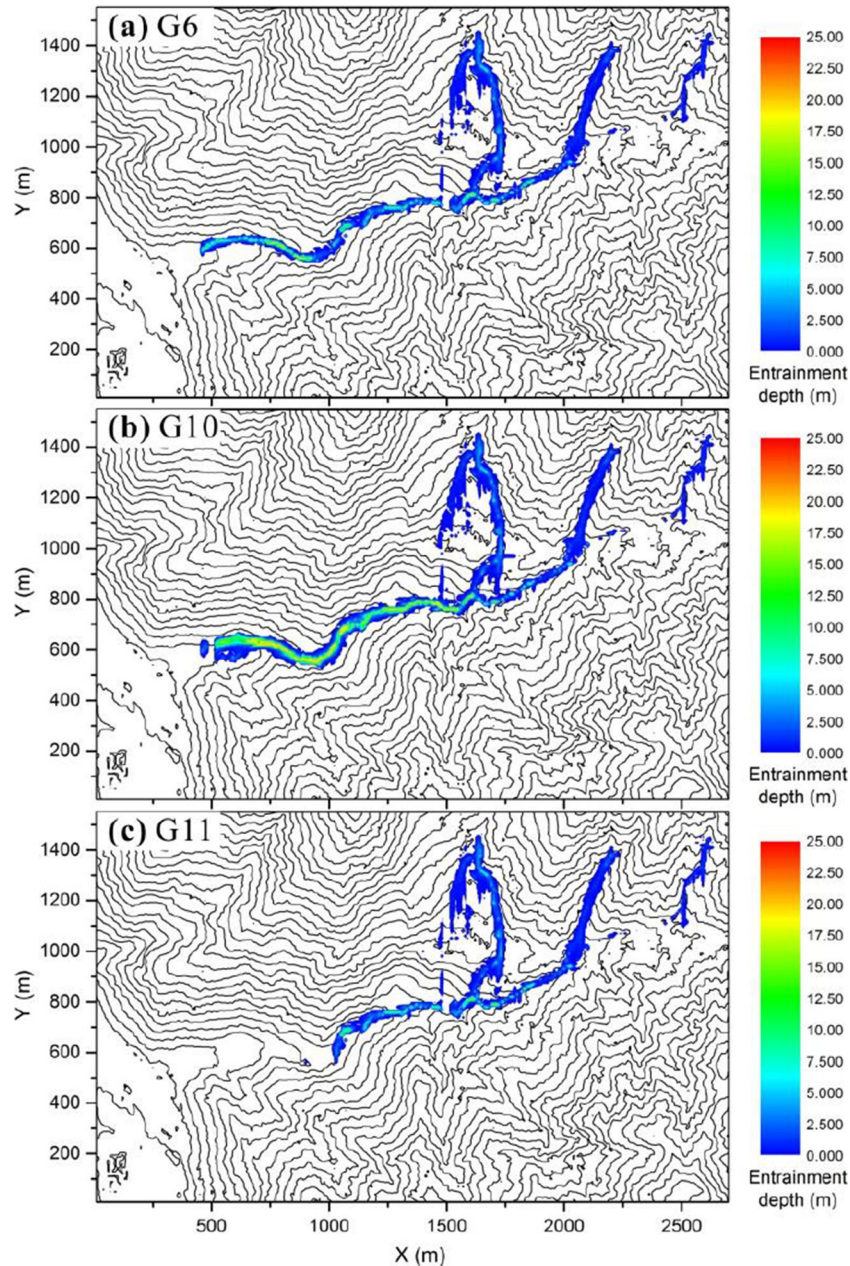


Fig. 12 Simulated entrainment depths in the catchment in G6, G10, and G11

Apart from that, this constraining effect delays the arrival time of the debris flow at downstream (P4), and it shows that the arrival time tends to be later when the check dam is constructed at upstream instead of at downstream. For example, the arrival time at P4 in G6 is 150.3 s, while those in G8 and G10 are 141.1 s and 116.1 s, respectively.

Some simulated characteristic data in all these simulation groups, including the entrainment volume, volume of the deposit rushing out the gully, and peak flow quantities and arrival times of the debris flow at the monitoring profiles, are provided in Table 5. These data agree well with the above analysis regarding to the simulation results with the effect of check dam.

Finally, the total volume evolution processes of the debris flow under the effect of bed entrainment in several different groups are compared in

Fig. 14. It also shows that the dam does have great influence on the entrainment rate of the debris flow. The groups constructing the check dams at the upper gully tend to have a smaller total volume of final debris deposit. In addition, the data in Table 5 show that those groups with less bed entrainment volume (or total volume) tend to have less debris mass rushing out the outlet of the gully.

Discussions

Twenty groups of simulations with different bed entrainment and check dam setups are conducted by using the improved model proposed in this paper. The debris flow event occurred in the Hongchun gully in 2010 is analyzed by the model, and the results of considering and not considering bed entrainment are compared. It shows that bed entrainment has a dominant influence on the final scale and dynamics

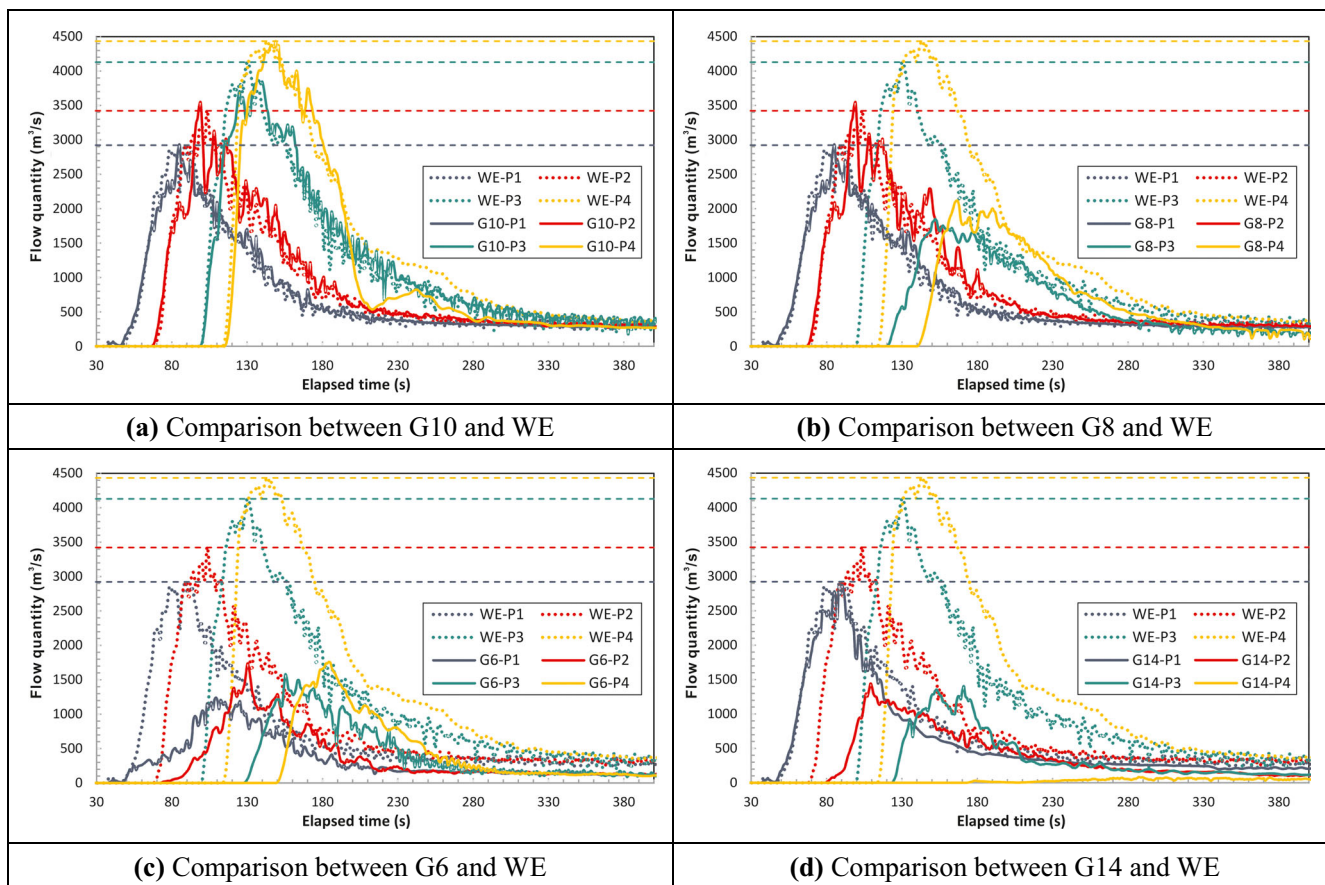


Fig. 13 Influence of check dam on the flow quantities at four profiles

of this debris flow. Without bed entrainment, this debris flow could not develop into a huge catastrophic event which blocked the Mingjiang River. The simulation result of considering bed entrainment matches quite well with the field data, demonstrating that the model performs well in modeling this debris flow. In addition, the scale of this debris flow and its flow quantity in the gully expand violently by entraining loose materials along the gully, so it is necessary to account for bed entrainment when designing check dams in this gully. Otherwise, the prevention effect of a check dam may be significantly overestimated, thus leading to an inadequate design of prevention measures. The results of those groups with check dams inside the gully indicate that the check dams can obviously alter the bed entrainment character and the dynamic process of this debris flow. The flow quantity at the downstream of the dam and the entrainment scale will be reduced greatly due to the impeding effect of the dam, while the arrival time at downstream of the gully will be delayed.

In the improved model, the effect of dam is taken as a velocity constraint which is imposed on the upstream cells next to the dam (Eq. (11)). Actually, the interactive process between a debris flow and a dam is much complicated. During the first few seconds when the debris flow impacts on the wall of the dam, it may produce a vertical jet-like bulge (Armanini 1997), or even be reflected back by the wall, turning the flow into a very complex turbulence. This phenomenon is important for analyzing the mechanical impact of the debris flow on structures (Wang et al. 2018), and need to be accounted when designing the structure strength of the check

dams. However, the main purpose of this paper is to study the prevention effect of check dam and its interactive influences with bed entrainment and the dynamics of a debris flow, so the check dams are simply taken as a rigid body here. Furthermore, although the vertical surging process may transport part of the debris mass over the check dam, the amount is quite limited because this process is usually very short. The main body will accumulate behind the dam until surpassing the top of the dam. Therefore, the rigid constraint assumption about the check dam is reasonable for the present study, and it shows a good numerical effect in reflecting the impeding effect of the check dams according to the simulation results. Comparing with some other widely used depth-averaged models (Hung and McDougall 2009; Ouyang et al. 2013; Pastor et al. 2009; Sassa et al. 2010), our model is similar to them in terms of the basic governing equations for depicting the run-out process of debris flows. However, these models are mainly designed to simulate and assess the run-out processes of rapid flow-like landslides on green field without artificial barriers, and the impeding effect of check dams cannot be properly reflected by them. By contrast, the improved model here introduces a rigid constraint condition to account for the effect of check dams, expanding the application range of the depth-averaged models from risk assessment to the design and assessment of check dams in debris flow gullies. Additionally, although a few other previous studies (Chen et al. 2019; Cuomo et al. 2019; Dai et al. 2017; Liu et al. 2013) have accounted for the effect of artificial barriers on the

Table 5 Simulation results of entrainment, deposition and flow characters at monitoring profiles in different groups

Simulation 7groups	Entrainment volume (m ³)	Deposit rushing out outlet(m ³)				Peak volume flow quantity (m ³ /s)				Arrival time of debris flow (s)			
		P1	P2	P3	P4	P1	P2	P3	P4	P1	P2	P3	P4
NE	0	35,000	1095	1055	778	743	46.6	78.5	117.5	140.5			
WE	580,000	349,000	2921	3422	4129	4432	35.5	68.4	99.2	114.2			
G0	0	2000	1097	182	50	49	47.5	125.4	187.4	239.4			
G1	466,000	241,000	1878	2348	2689	3053	37.5	71.3	106.2	123.2			
G2	515,000	266,000	2993	2865	2893	3103	35.5	71.3	103.2	119.2			
G3	539,000	287,000	2921	3381	3481	3328	35.5	68.4	103.2	118.2			
G4	515,000	235,000	2921	3422	3947	2793	35.5	68.4	99.2	116.1			
G5	552,000	234,000	2921	3422	4129	4468	35.5	68.4	99.2	114.1			
G6	272,000	92,000	1240	1739	1577	1761	37.5	72.3	128.3	150.3			
G7	334,000	103,000	2875	1442	1345	1489	36.5	80.2	124.1	143.2			
G8	458,000	171,000	2928	3543	1848	2114	36.5	67.3	119.1	141.1			
G9	442,000	129,000	2928	3544	3983	1341	36.5	67.3	99.2	125.1			
G10	543,000	50,000	2928	3544	3864	4434	36.5	67.3	99.2	116.1			
G11	187,000	9000	1240	1724	203	141	37.5	72.3	195.3	235.3			
G12	214,000	5000	1240	1739	1464	78	37.5	72.3	128.3	174.3			
G13	263,000	11,000	1240	1739	1577	1754	37.5	72.3	128.3	150.3			
G14	271,000	10,000	2875	1442	1402	83	36.5	80.2	124.2	174.2			
G15	324,000	13,000	2875	1442	1361	1613	36.5	80.2	124.2	144.2			
G16	428,000	16,000	2928	3541	2056	2203	36.5	67.3	119.1	140.1			
G17	187,000	1000	1240	1724	203	141	37.5	72.3	195.3	235.3			

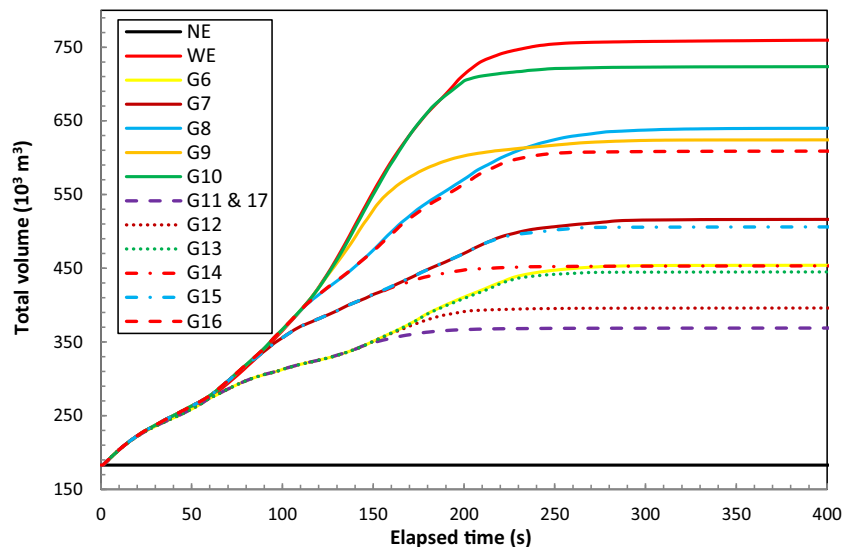


Fig. 14 Simulated total volume evolution curves of the debris flow in different groups

dynamics of flow-like landslides, they did not consider bed entrainment or did not account for its interactive effects with check dams. Therefore, this paper is also helpful in better understanding the effects of check dams on the bed entrainment and dynamic processes of debris flows. Another improvement adopted in this paper regarding computational scheme performs well in promoting computational efficiency. In some models (Sassa et al. 2010), the computational region is a fixed rectangular area with debris flows run inside it, while in some other models (Liu and Huang 2006; Ouyang et al. 2013; Shen et al. 2018a) the computational region is a dynamic rectangular area whose size changes with the propagation of debris flows. In both cases, plenty of empty cells will involve in the calculation, resulting in the waste of a great amount of computational time. In comparison, the improved computation method adopted here only calculates the cells with debris mass in them, so that it can greatly reduce the computational cost. The total computational time for calculating 50,000 time steps in simulating the present debris flow (cell numbers are 41,850) is about 3 h and 15 min, while the time consumption is more than 6 times (20 h and 40 min) of the new scheme if the old scheme (Ouyang et al. 2013, Shen et al. 2018a) is adopted. These two improvements make the new model more suitable for modeling the dynamic process of a long run-out debris flow with obviously bed entrainment phenomenon and check dams in the gully. The current simulations were conducted on an ordinary desktop with a CPU produced by Intel (Intel (R) Core (TM) i7-4770 @ 3.40 GHz). The computation time can be further reduced by adopting high-performance server with better CPU or adopting parallel computing techniques, which will not be addressed this paper.

On the other hand, since the interaction between debris flows and check dams is a very complex phenomenon, it is still far from being fully understood currently. For instance, it is possible that the property (i.e., bulk density, components, and rheology) of a debris flow will change after surpassing a check dam. Such a complex process is very difficult to consider in a numerical model, so in the present study it is neglected for simplicity. The phenomena such as the property change of a debris flow due to the filtering effect of check dams are out of the scope of this paper, while further researches about them are needed in the future in order to improve the applicability of this model.

Conclusions

An improved numerical model is proposed in this paper to study the influence of check dams on the dynamic and bed entrainment processes of debris flow. The run-out process of the 2010 catastrophic Hongcuan gully debris flow is simulated by the new model, and the effects of check dams on the dynamic and bed entrainment processes of this debris flow are analyzed. The simulation results are presented and discussed, and following conclusions can be obtained.

- (1). Bed entrainment plays a dominant role in the formational and run-out processes of the Hongchun gully debris flow. Without bed entrainment, this debris flow could not evolve into a huge debris flow that blocked the Mingjiang River. The simulation results of the debris flow when considering bed entrainment agree well with the field data, indicating that the improved model has good numerical accuracy in modeling this debris flow.
- (2). Bed entrainment significantly alters the flow characters of this debris flow. Without bed entrainment, the peak value of flow quantity tends to decrease gradually from the upstream of the gully to the downstream, while the peak value will show an opposite tendency if bed entrainment is significant. Therefore, bed entrainment should be considered in assessing the prevention effect of check dams to prevent inadequate design of them.
- (3). Check dams can greatly change the dynamic and bed entrainment processes of this debris flow. They reduce the flow quantity and bed entrainment scale of the debris flow at the downstream side of the check dam, delaying the arrival time of the debris flow at downstream. Additionally, by effectively constraining the bed entrainment scale, the prevention effect of check dams tends to be better when they are constructed at the upper part of the gully.
- (4). The improved model is shown to be able to properly reflect the impeding effect of check dams, and the new computational scheme adopted in this model can significantly

improve the computation efficiency. These improvements make the present model more suitable in assessing the prevention effect of check dams on huge debris flows with obvious bed entrainment phenomenon.

Acknowledgments

We would like to thank the anonymous referees for careful reading the manuscript and providing insightful comments to help us improve the quality of this paper.

Funding information

This research is funded by the National Key R&D Program of China (Grant No. 2017YFC1501000, 2017YFC1501302), the Natural Science Foundation of China (Grant No. 41790433, 41877266), the State Key Laboratory of Geohazard Prevention and Geo-environment Protection Independent Research Project (Grant No. SKLGP2016Z014), and the China Scholarship Council (CSC) — University of Bologna Joint Scholarship (File No. 201806560011).

References

- Armanini A (1997) On the dynamic impact of debris flows. In: Armanini A, Michiue M (eds) Recent developments on debris flows. Springer, Berlin Heidelberg, pp 208–226. <https://doi.org/10.1007/BFb0117770>
- Berti M, Simoni A (2005) Experimental evidences and numerical modelling of debris flow initiated by channel runoff. *Landslides* 2:171–182. <https://doi.org/10.1007/s10346-005-0062-4>
- Chen X, Cui P, You Y, Chen J, Li D (2015) Engineering measures for debris flow hazard mitigation in the Wenchuan earthquake area. *Eng Geol* 194:73–85. <https://doi.org/10.1016/j.enggeo.2014.10.002>
- Chen H-X, Li J, Feng S-J, Gao H-Y, Zhang D-M (2019) Simulation of interactions between debris flow and check dams on three-dimensional terrain. *Eng Geol* 251:48–62. <https://doi.org/10.1016/j.enggeo.2019.02.001>
- Crosta GB, Imposimato S, Roddeman D (2009) Numerical modelling of entrainment/deposition in rock and debris-avalanches. *Eng Geol* 109:135–145. <https://doi.org/10.1016/j.enggeo.2008.10.004>
- Cui P, Chen X-Q, Zhu Y-Y, Su F-H, Wei F-Q, Han Y-S, Liu H-J, Zhuang J-Q (2011) The Wenchuan earthquake (may 12, 2008), Sichuan province, China, and resulting geohazards. *Nat Hazards* 56:19–36. <https://doi.org/10.1007/s11069-009-9392-1>
- Cui P, Zeng C, Lei Y (2015) Experimental analysis on the impact force of viscous debris flow. *Earth Surf Process Landf* 40:1644–1655. <https://doi.org/10.1002/esp.3744>
- Cuomo S, Pastor M, Capobianco V, Cascini L (2016) Modelling the space–time evolution of bed entrainment for flow-like landslides. *Eng Geol* 212:10–20. <https://doi.org/10.1016/j.enggeo.2016.07.011>
- Cuomo S, Moretti S, Aversa S (2019) Effects of artificial barriers on the propagation of debris avalanches. *Landslides* 16:1077–1087. <https://doi.org/10.1007/s10346-019-01155-1>
- Dai Z, Huang Y, Cheng H, Xu Q (2017) Sph model for fluid–structure interaction and its application to debris flow impact estimation. *Landslides* 14:917–928. <https://doi.org/10.1007/s10346-016-0777-4>
- Evans SG, Tutubalina OV, Drobyshev VN, Chernomoretz SS, McDougall S, Petrakov DA, Hungr O (2009) Catastrophic detachment and high-velocity long-runout flow of Kolka Glacier, caucasus mountains, Russia in 2002. *Geomorphology* 105:314–321. <https://doi.org/10.1016/j.geomorph.2008.10.008>
- Fracarollo L, Capart H (2002) Riemann wave description of erosional dam-break flows. *J Fluid Mech* 461:183–228. <https://doi.org/10.1017/S0022112002008455>
- Frank F, McArdell BW, Huggel C, Vieli A (2015) The importance of entrainment and bulking on debris flow runout modeling: examples from the swiss alps. *Nat Hazards Earth Syst Sci* 15:2569–2583. <https://doi.org/10.5194/nhess-15-2569-2015>
- Gao L, Zhang LM, Chen HX (2017) Two-dimensional simulation of debris flow impact pressures on buildings. *Eng Geol* 226:236–244. <https://doi.org/10.1016/j.enggeo.2017.06.012>
- García-Martínez R, López JL (2005) Debris flows of december 1999 in Venezuela. In: Debris-flow hazards and related phenomena. Springer, Berlin Heidelberg, pp 519–538. https://doi.org/10.1007/3-540-27129-5_20
- Hu W, Dong XJ, Xu Q, Wang GH, van Asch TWJ, Hicher PY (2016) Initiation processes for run-off generated debris flows in the wenchuan earthquake area of China. *Geomorphology* 253:468–477. <https://doi.org/10.1016/j.geomorph.2015.10.024>
- Huang R, Li W (2014) Post-earthquake landsliding and long-term impacts in the Wenchuan earthquake area, China. *Eng Geol* 182:111–120. <https://doi.org/10.1016/j.enggeo.2014.07.008>
- Huang Y, Cheng H, Dai Z, Xu Q, Liu F, Sawada K, Moriguchi S, Yashima A (2015) Sph-based numerical simulation of catastrophic debris flows after the 2008 Wenchuan earthquake. *Bull Eng Geol Environ* 74:1137–1151. <https://doi.org/10.1007/s10064-014-0705-6>
- Hungr O, Evans SG (2004) Entrainment of debris in rock avalanches: an analysis of a long run-out mechanism. *GSA Bull* 116:1240–1252. <https://doi.org/10.1130/B25362.1>
- Hungr O, McDougall S (2009) Two numerical models for landslide dynamic analysis. *Comput Geosci* 35:978–992. <https://doi.org/10.1016/j.cageo.2007.12.003>
- Hungr O, Leroueil S, Picarelli L (2014) The Varnes classification of landslide types, an update. *Landslides* 11:167–194. <https://doi.org/10.1007/s10346-013-0436-y>
- Iverson RM (2012) Elementary theory of bed-sediment entrainment by debris flows and avalanches. *J Geophys Res Earth Surf* 117:F03006. <https://doi.org/10.1029/2011JF002189>
- Iverson RM, Ouyang C (2015) Entrainment of bed material by earth-surface mass flows: review and reformulation of depth-integrated theory. *Rev Geophys* 53:27–58. <https://doi.org/10.1002/2013RG000447>
- Iverson RM, Reid ME, LaHusen RG (1997) Debris-flow mobilization from landslides. *Annu Rev Earth Planet Sci* 25:85–138. <https://doi.org/10.1146/annurev.earth.25.1.85>
- Iverson RM, Reid ME, Logan M, LaHusen RG, Godt JW, Griswold JP (2010) Positive feedback and momentum growth during debris-flow entrainment of wet bed sediment. *Nat Geosci* 4:116–121. <https://doi.org/10.1038/ngeo1040>
- Jakob M, Hungr O (2005) Introduction. In: Debris-flow hazards and related phenomena. Springer, Berlin Heidelberg, pp 1–7. https://doi.org/10.1007/3-540-27129-5_1
- Kattel P, Kafle J, Fischer J-T, Mergili M, Tuladhar BM, Pudasaini SP (2018) Interaction of two-phase debris flow with obstacles. *Eng Geol* 242:197–217. <https://doi.org/10.1016/j.enggeo.2018.05.023>
- Liu W, He S (2016) A two-layer model for simulating landslide dam over mobile river beds. *Landslides* 13:565–576. <https://doi.org/10.1007/s10346-015-0585-2>
- Liu K-F, Huang MC (2006) Numerical simulation of debris flow with application on hazard area mapping. *Comput Geosci* 10:221–240. <https://doi.org/10.1007/s10596-005-9020-4>
- Liu J, Nakatani K, Mizuyama T (2013) Effect assessment of debris flow mitigation works based on numerical simulation by using kanako 2d. *Landslides* 10:161–173. <https://doi.org/10.1007/s10346-012-0316-x>
- Liu W, He S, Li X, Xu Q (2016) Two-dimensional landslide dynamic simulation based on a velocity-weakening friction law. *Landslides* 13:957–965. <https://doi.org/10.1007/s10346-015-0632-z>
- McDougall S, Hungr O (2005) Dynamic modelling of entrainment in rapid landslides. *Can Geotech J* 42:1437–1448. <https://doi.org/10.1139/t05-064>
- Ouyang C, He S, Xu Q, Luo Y, Zhang W (2013) A maccormack-tvd finite difference method to simulate the mass flow in mountainous terrain with variable computational domain. *Comput Geosci* 52:1–10. <https://doi.org/10.1016/j.cageo.2012.08.024>
- Ouyang C, He S, Tang C (2015) Numerical analysis of dynamics of debris flow over erodible beds in Wenchuan earthquake-induced area. *Eng Geol* 194:62–72. <https://doi.org/10.1016/j.enggeo.2014.07.012>
- Parker RN, Densmore AL, Rosser NJ, de Michele M, Li Y, Huang R, Whadcoat S, Petley DN (2011) Mass wasting triggered by the 2008 Wenchuan earthquake is greater than orogenic growth. *Nat Geosci* 4:449–452. <https://doi.org/10.1038/ngeo1154>
- Pastor M, Haddad B, Sorbino G, Cuomo S, Drempetic V (2009) A depth-integrated, coupled SPH model for flow-like landslides and related phenomena. *Int J Numer Anal Methods Geomech* 33:143–172. <https://doi.org/10.1002/nag.705>
- Pirulli M, Pastor M (2012) Numerical study on the entrainment of bed material into rapid landslides. *Géotechnique* 62:959–972. <https://doi.org/10.1680/geot.10.P.074>
- Pitman EB, Le L (2005) A two-fluid model for avalanche and debris flows. *Philos Trans R Soc A Math Phys Eng Sci* 363:1573–1601. <https://doi.org/10.1098/rsta.2005.1596>
- Ren D (2014) The devastating zhouqu storm-triggered debris flow of august 2010: likely causes and possible trends in a future warming climate. *J Geophys Res-Atmos* 119:3643–3662. <https://doi.org/10.1002/2013jd020881>
- Sassa K, Nagai O, Solidum R, Yamazaki Y, Ohta H (2010) An integrated model simulating the initiation and motion of earthquake and rain induced rapid landslides and its

- application to the 2006 Leyte landslide. *Landslides* 7:219–236. <https://doi.org/10.1007/s10346-010-0230-z>
- Savage SB, Hutter K (1989) The motion of a finite mass of granular material down a rough incline. *J Fluid Mech* 199:177–215. <https://doi.org/10.1017/S0022112089000340>
- Scott KM, Macias JL, Naranjo JA, Rodriguez S and McGeehin JP (2001) Catastrophic debris flows transformed from landslides in volcanic terrains: mobility, hazard assessment and mitigation strategies. Professional paper, – edn., doi: <https://doi.org/10.3133/pp1630>
- Shen W, Li T, Li P, Guo J (2018a) A modified finite difference model for the modeling of flowslides. *Landslides* 15:1577–1593. <https://doi.org/10.1007/s10346-018-0980-6>
- Shen W, Li T, Li P, Shen Y, Lei Y, Guo J (2018b) The influence of the bed entrainment-induced rheology and topography changes on the propagation of flow-like landslides: a numerical investigation. *Bull Eng Geol Environ*. <https://doi.org/10.1007/s10064-018-01447-1>
- Takahashi T (2009) A review of Japanese debris flow research. *Int J Eros Cont Eng* 2:1–14. <https://doi.org/10.13101/ijece.2.1>
- Tang C, Zhu J, Ding J, Cui XF, Chen L, Zhang JS (2011) Catastrophic debris flows triggered by a 14 august 2010 rainfall at the epicenter of the Wenchuan earthquake. *Landslides* 8:485–497. <https://doi.org/10.1007/s10346-011-0269-5>
- Tang C, van Asch TWJ, Chang M, Chen GQ, Zhao XH, Huang XC (2012a) Catastrophic debris flows on 13 august 2010 in the qingping area, southwestern China: the combined effects of a strong earthquake and subsequent rainstorms. *Geomorphology* 139–140:559–576. <https://doi.org/10.1016/j.geomorph.2011.12.021>
- Tang C, Zhu J, Chang M, Ding J, Qi X (2012b) An empirical–statistical model for predicting debris-flow runout zones in the Wenchuan earthquake area. *Quat Int* 250:63–73. <https://doi.org/10.1016/j.quaint.2010.11.020>
- Wang D, Chen Z, He S, Liu Y, Tang H (2018) Measuring and estimating the impact pressure of debris flows on bridge piers based on large-scale laboratory experiments. *Landslides* 15:1331–1345. <https://doi.org/10.1007/s10346-018-0944-x>
- Xu Q, Zhang S, Li W, Van Asch TW (2012) The 13 august 2010 catastrophic debris flows after the 2008 Wenchuan earthquake, China. *Nat Hazards Earth Syst Sci* 12:201–216. <https://doi.org/10.5194/nhess-12-201-2012>

W. Shen · D. Wang (✉) · **H. Qu**

State Key Laboratory of Geohazard Prevention and Geoenvironment Protection, Chengdu University of Technology, Chengdu, 610059, Sichuan, China
Email: wangdongpo2014@cdut.edu.cn

W. Shen

e-mail: shenweichd@qq.com

H. Qu

e-mail: 871781461@qq.com

W. Shen

Department of Biological, Geological and Environmental Sciences, University of Bologna, 40126, Bologna, Italy

T. Li

Department of Geological Engineering, Chang'an University, Xi'an, 710054, China
e-mail: dcdgx08@chd.edu.cn